

Biodegradable Shape-Memory Polymer Networks: Characterization with Solid-State NMR

Marko Bertmer,^{*,†} Alina Buda,[†] Iris Blumenkamp-Höfges,[‡] Steffen Kelch,[‡] and Andreas Lendlein^{*}

Institute of Technical and Macromolecular Chemistry, Worringer Weg 1, 52056 Aachen, Germany, and GKSS Research Center Geesthacht GmbH, Kantstrasse 55, 14513 Teltow, Germany

Received January 24, 2005; Revised Manuscript Received February 25, 2005

ABSTRACT: Polymer networks made from oligo[(L-lactide-*ran*-glycolide)]dimethacrylates by UV curing are characterized by solid-state NMR. These polymer networks show a shape-memory effect and could be used as temporary implant materials for medical applications. The ^{13}C spectra enable the direct determination of the cross-link density by a signal at 44 ppm. This is used to correlate its intensity with the chain segment length as well as to study the kinetics of photo-cross-linking. The latter is compared with the gel content, and it is found that the NMR method detects the real amount of covalent cross-links whereas the gel content also depends on influences from constraints such as physical entanglements. The shape-memory effect of the polymer networks can be followed as well by ^1H double quantum buildup curves of samples that are programmed by stretching. Results indicate the reversibility of the shape-memory process.

1. Introduction

In medicine there is an increasing demand for different types of implant materials. Several types of materials, mainly polymers, are already in use or are being tested for their biocompatibility and functionality.¹ One path follows the research for temporarily implanted materials that degrade in the body to nontoxic products after a time that can be tailored for a certain application. In this way, no further surgery is necessary to remove the implant after fulfilling its temporary purpose, and long-term complications can be avoided. Implant materials based on synthetic, hydrolytically degradable polymers have led to dramatic progress in a variety of medical treatments.^{2–4} A field, in which shape-memory polymers could be an enabling technology for future applications, is minimally invasive surgery.^{5,6} On the basis of noncrystallizable switching segments, completely amorphous shape-memory polymer networks having a glass transition temperature as transition temperature (T_{trans}) can be designed.⁷ Those networks are transparent, and it is expected that they show a more homogeneous degradation than semicrystalline polymers since hydrolytic degradation occurs faster in amorphous regions than in crystalline ones. The homogeneous degradation behavior of amorphous aliphatic copolyesters qualifies them also as preferred matrices in the area of controlled drug delivery.^{8–12}

We present experimental data on the solid-state NMR characterization of covalently cross-linked polymer networks based on random copolymers of LL-dilactide and diglycolide. Rather short chain segment lengths below or equal to a number-average molecular weight M_n of 10 000 g mol⁻¹ were employed. These oligomers contain methacrylate end groups at both chain ends that are cross-linked by UV light without using a photoinitiator. The polymer networks obtained in this way are fully amorphous and exhibit a thermally induced shape-

memory effect.^{13,14} In these amorphous polymer networks a certain shape can be programmed by heating the sample above the glass transition temperature (T_g) of the oligo(L-lactide-*ran*-glycolide) chain segments and fixed by cooling below T_g . The obtained macroscopic shape is called temporary shape. Upon reheating above T_g , the permanent shape is recovered driven by the entropy elasticity of the elastomeric polymer network.^{15,16}

The chemical and physical characterization of these polymer networks is not straightforward. Because of their insolubility, solid-state characterization techniques are important. For these amorphous systems, it is demonstrated that solid-state NMR is a very versatile tool to get information about the molecular architecture of the polymer network. We present data based on ^{13}C measurements regarding questions about chemical composition, cross-link density, and optimum UV curing time. The quaternary carbon signal of poly(methacrylate) created by the cross-linking is well separated in the ^{13}C spectrum so that a direct access to the cross-link density is possible by simple integration. As a demonstration that the shape-memory effect can also be monitored by solid-state NMR, we present results of ^1H double quantum experiments comparing programmed and unprogrammed samples before and after heating above T_g . This shape-memory behavior was investigated with regard to the efficiency of the recovery of the permanent shape for samples stretched by a maximum elongation of 80%. To our knowledge, this represents the first NMR investigation of the shape-memory effect in polymer networks. The investigation of changes in NMR parameters as a function of temperature and the degradation of these polymer networks under physiological conditions followed with different solid-state NMR methods will be presented in an upcoming publication.¹⁷

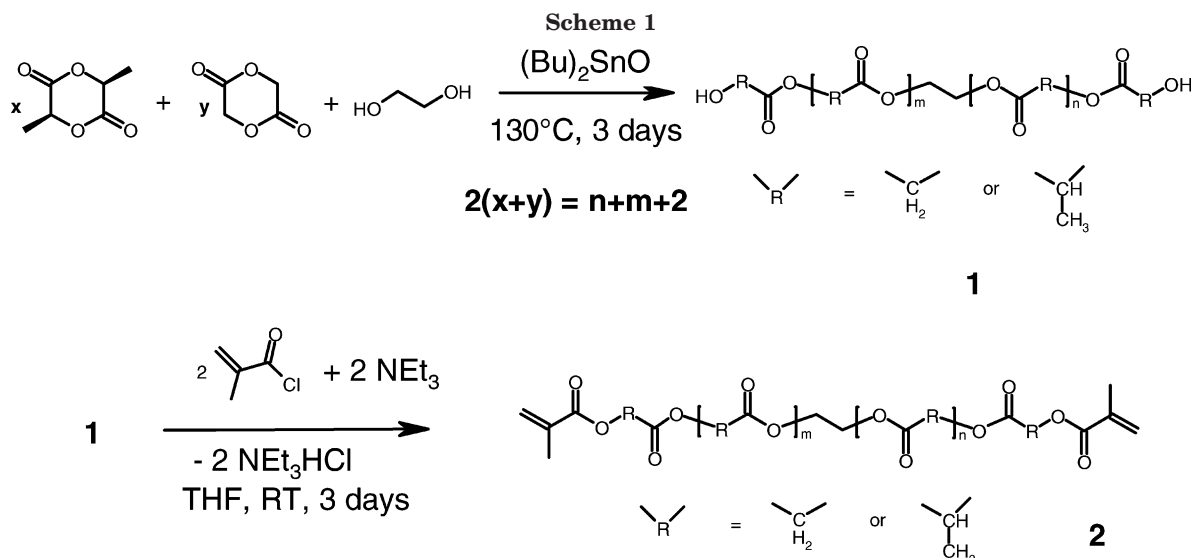
2. Experimental Section

2.1. Samples. For a detailed description of the synthesis of the polymer networks, the reader is referred to an upcoming

[†] Institute of Technical and Macromolecular Chemistry.

[‡] GKSS Research Center Geesthacht GmbH.

* Corresponding author. E-mail: mbertmer@mc.rwth-aachen.de.



publication.¹³ Scheme 1 shows the general reaction scheme starting from LL-dilactide and diglycolide. The macrodiol **1** is obtained by ring-opening polymerization of LL-dilactide and diglycolide, using ethylene glycol as the initiator and dibutyltin oxide as a catalyst. The catalyst promotes transesterification, the extent of which depends on reaction time and temperature. The optimum reaction time was determined by measuring ¹H NMR solution spectra at different reaction times and analyzing the relative content of pentades with different amounts of lactide and glycolide.^{14,24} *M_n* is controlled by the chosen molar ratio of monomer to initiator and was determined from ¹H solution NMR. The conversion of the reaction is higher than 85%. Residual monomers are removed by precipitating the copolymer. Polydispersities are in the range of 1.4 and were determined from gel permeation chromatography (GPC), done with a mixed D column (600 mm × 7.5 mm, Polymer Laboratories Ltd.) and an RI detector (ERC Inc.). Chloroform was used as an eluent at a flow rate of 1 mL/min at room temperature. Calibration was done with polystyrene standards.

By end-group functionalization of the macrodiols with methacryloyl chloride the macrodimethacrylates **2** are obtained. Polymer networks with different chain segment lengths of the dimethacrylates and different comonomer ratios were synthesized. The macrodimethacrylates **2** are molten and cast into films prior to the UV irradiation. Photocuring was performed without a photoinitiator with a Fusion UV system F300 M (Fusion UV, Gaithersburg, MD) equipped with a high-pressure mercury lamp (1800 W). The distance between lamp head and sample was 25 cm. Because of the thermal radiation of the lamp, the polymer melt had a temperature of 90 °C during photopolymerization, with a light intensity of about 120 W cm⁻². Samples were usually photoirradiated for 25 min. This time was determined in preexperiments from both the disappearance of the IR band of the double bond at 1637 cm⁻¹ and the determination of the gel content (see below). The results of the ¹³C CPMAS experiments are described below. After curing, samples are swollen in chloroform to remove unreacted macrodimethacrylates and dried until constant weight is reached prior to the NMR measurements. The resulting polymer networks are hard and fairly brittle.

Differential scanning calorimetry (DSC) measurements indicated that all samples were completely amorphous. Figure 1 shows exemplified the DSC spectrum after the second heating run of a polymer network with a chain segment length of 5700 g mol⁻¹; *T_g* is 54 °C obtained with a heating rate of 10 K/min. The *T_g* values of the polymer networks are in the range between 50 and 55 °C and are fairly independent of the molecular weight of the network precursor. For longer chain segments the *T_g* values are slightly higher.

2.2. NMR Measurements. Experiments were performed on a Bruker Avance DSX 500 spectrometer with frequencies

of 500.46 and 125.84 MHz for ¹H and ¹³C, respectively. A 7 mm MAS probe was used for both static and MAS measurements. For the latter, a spinning speed of 5 kHz was used unless otherwise stated. $\pi/2$ pulse lengths were about 5 μ s for both the ¹H and ¹³C channel. The standard CPMAS sequence¹⁸ was taken with TPPM decoupling.¹⁹ Typical measurement parameters were a recycle delay of 5 s and a contact time of 2 ms. For the dipolar dephasing experiment,^{20–23} the method of Opella and Frey²⁰ with a delay time without proton decoupling of 40 μ s was employed. Spectra were referenced externally to tetramethylsilane (TMS).

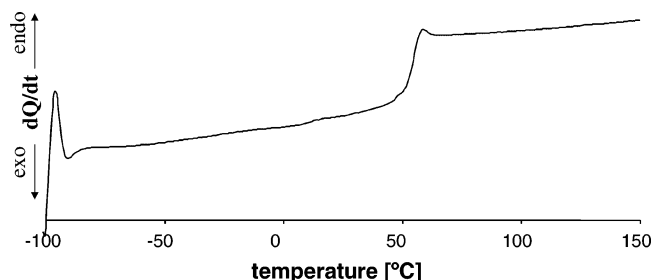


Figure 1. DSC spectrum of a polymer network with a chain segment length of 5700 g mol⁻¹ and a copolymer molar ratio of 71:29 LL-dilactide to diglycolide.

3. Results and Discussion

3.1. Characterization of Precursors and Polymer Networks. As a first step, the complete assignment of the ¹³C spectra of the polymer network and the reaction precursors was made. Figure 2 shows the ¹³C CPMAS spectra of the macrodiol **1** and the macrodimethacrylate **2** as well as the polymer network with chain segment *M_n* of 4400 g mol⁻¹ measured with similar parameters. The main signals from the poly(L-lactide-*ran*-glycolide) segments with chemical shifts of 17 ppm for the methyl group of lactide, 61 ppm for the methylene group of glycolide, 69 ppm for the methine group of lactide, and of 170 ppm for the carbonyl carbons are present in all samples. The rather high line widths of these signals and the fact that for some signals an additional shoulder is visible has its origin in a distribution of chemical shifts. This is because in the randomized sequence structure a variety of different combinations of lactide and glycolide monomer units are present. It was shown in solution NMR where analysis was based on pentades that copolymers of LL-dilactide and diglycolide give rise to chemical shifts in a fairly broad shift range.^{24–26} The

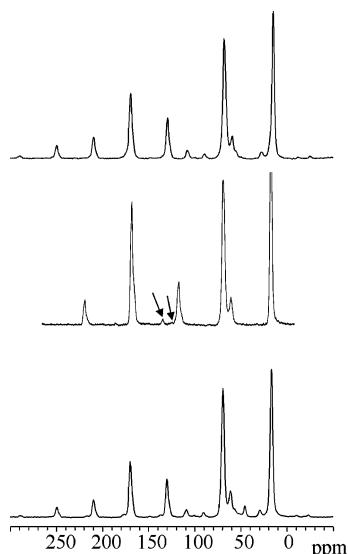


Figure 2. ^{13}C CPMAS spectra of macrodiol **1** (top), macrodimethacrylate **2** (middle), and polymer network (bottom) with a chain segment length of 4400 g mol^{-1} . Spinning speed is 5 kHz for the macrodiol **1** and the polymer network and 6 kHz for the macrodimethacrylate **2**. The arrows point at the small signal intensity of the two olefinic carbon signals of the dimethacrylate.

Table 1. ^{13}C Chemical Shifts of the Polymer Network

^{13}C chemical shift [ppm]	assignment of functional group
17	methyl groups of lactide and methacrylate
44	quaternary carbons of methacrylate
52	methylene carbons of methacrylate
61	methylene carbons of glycolide
69	methine carbons of lactide
170	carbonyl carbons of lactide and glycolide
177	carbonyl carbons of methacrylate

olefinic carbons of the macrodimethacrylate **2** have chemical shifts of 136 and 125 ppm, whereas the signal at 125 ppm is barely visible.²⁷ The spectrum was obtained at 6 kHz spinning speed instead of 5 kHz to avoid overlap with a spinning sideband of the carbonyl carbons. The olefinic carbon signals of the dimethacrylate are rather weak because of the low amount of olefinic carbons within the chain. Additionally, because of the higher degree of orientational freedom, a larger distribution of chemical shifts is present, leading to less pronounced signals especially for the 125 ppm signal. The higher mobility also reduces the cross-polarization efficiency and further reduces the signal intensity of the olefinic carbon signals. The other signals of the methacrylate end group are obscured by the already present signals of lactide and glycolide units (168 ppm for the carbonyl carbon and 18 ppm for the methyl carbon). Signals of the olefinic carbons disappear to the same extent as the double bonds react during the UV curing process to yield a poly(methacrylate) backbone linked by the poly(L-lactide-*ran*-glycolide) segments. Signals arise at 177 ppm due to the carbonyl carbon of the poly(methacrylate) group, at 52 ppm for the methylene, and at 44 ppm for the quaternary carbon.²⁸ However, the methylene carbon signal at 52 ppm is visible as a shoulder only. The complete assignment of the signals for the polymer network is summarized in Table 1. All other signals present in the solid-state spectra are due to spinning sidebands because the spinning rate is smaller than the chemical shift anisotropy of the individual carbons. The rather large intensities of the

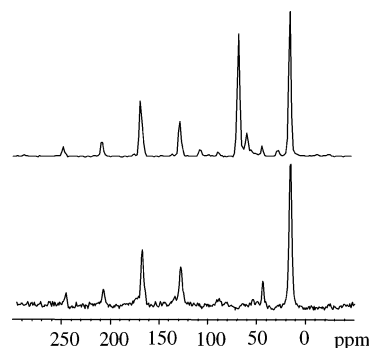


Figure 3. ^{13}C CPMAS (top) and dipolar dephasing spectrum (bottom) of the polymer network with a chain segment length of 4400 g mol^{-1} . The dephasing period was set to $40\text{ }\mu\text{s}$.

spinning sidebands—especially for the carbonyl carbons—also indicate that the polymer networks are fairly rigid systems and exhibit only low mobility.

For further clarification about the assignment of the 44 ppm signal, a dipolar dephasing experiment was performed; the result is shown in Figure 3. In this experiment, a delay after the contact pulse is inserted prior to data acquisition; in our case it was set to $40\text{ }\mu\text{s}$. During this period without proton decoupling the magnetization of those carbons strongly coupled to protons dephases leaving over only the signals from the weaker coupled carbons like nonprotonated carbons and carbons with high mobility such as methyl groups that exhibit fast rotations around the 3-fold axis. The results are clearly visible from Figure 3. Only the signals from the carbonyl carbon, the methyl carbons, and the signal at 44 ppm are present. This confirms our assignment that the 44 ppm signal originates from the quaternary carbon of the methacrylate group after cross-linking. Furthermore, this signal is well separated from all other signals in the spectrum and therefore enables the direct determination of the cross-link density by simple signal integration, which will be employed in the next paragraphs.

3.2. Investigation of Polymer Networks with Different Comonomer Ratios. As a second step, the characterization of samples with different comonomer ratios was performed. Samples with comonomer weight ratios of LL-dilactide to diglycolide of 85:15, 75:25, and 60:40 were synthesized. Together with their molecular weights, this leads to molar ratios of 82:18, 71:29, and 55:45, respectively. The resulting ^{13}C CPMAS spectra are shown in Figure 4. The different comonomer ratios are visible by the changes in the signal intensities of the methine groups of lactide at 69 ppm and of the methylene groups of glycolide at 61 ppm. With increasing glycolide content the signal intensity of the 61 ppm signal increases. On the basis of the integral intensity of these two signals, the stoichiometric ratio of the two monomer units can be calculated. The results are summarized in Table 2. Solution ^1H NMR of the dimethacrylate precursor gave identical values for the lactide-to-glycolide ratio as the calculated ones from synthesis input. Also, a good agreement between the calculated ratios and those determined from ^{13}C CPMAS exists, which demonstrates that this analysis is justified. This cannot always be expected because CPMAS intensities are in general not quantitative. Nevertheless, the methylene and methine carbons have a similar contact time behavior so that their relative intensities are fairly constant as confirmed by determining the relative

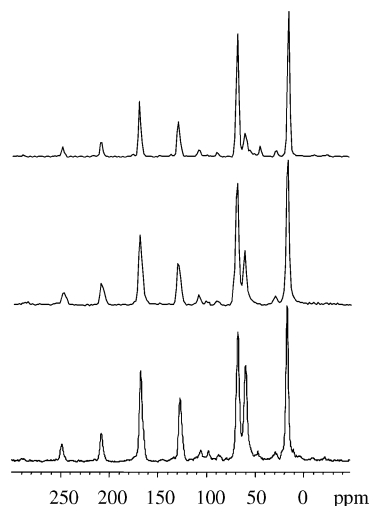


Figure 4. ^{13}C CPMAS spectra of polymer networks with different comonomer ratios: top, lactide-to-glycolide molar ratio 82:18 (chain segment M_n of methacrylate precursor 6500 g mol^{-1}); middle, 71:29 (5700 g mol^{-1}); bottom, 55:45 (6800 g mol^{-1}).

Table 2. Molar Ratios of L-Lactide and Glycolide in the Copolymer Chain Segments As Determined from ^{13}C CPMAS Measurements Compared to the Relative Amounts of LL-Dilactide and Diglycolide from Synthesis Input

according to synthesis input	calculated from NMR data
82:18	84:16
71:29	74:26
55:45	58:42

intensities at different contact times (data not shown). Unexpectedly, slightly higher relative intensities are determined for the lactide signal. In general, the copolymerization reaction kinetics favors the addition of a glycolide unit to the growing polymer chain.²⁹ As a consequence, one would expect a slightly higher signal intensity for the glycolide signal. From our analysis in comparison to solution NMR data from the dimethacrylate precursor, however, this effect is not observed.

3.3. Determination of the Cross-Link Density. Because of the fact that the signal at 44 ppm originates from the quaternary carbon in poly(methacrylate) as a product of UV cross-linking and is well separated from the other signals in the ^{13}C spectrum, its signal intensity is a direct measure of the cross-link density. Six polymer networks with chain segment number-average molecular weights M_n between 1000 and 10 000 g mol^{-1} —as determined from ^1H solution NMR of the dimethacrylate precursor—were analyzed. Figure 5 shows a stack plot of the CPMAS spectra of three representative polymer network samples recorded under identical measurement conditions. The signal intensity of the 44 ppm signal is increasing with decreasing segment chain length, i.e., increasing cross-link density. In analogy the intensities of the other carbon signals of the methacrylate unit, the 177 ppm signal of the carbonyl carbon and the 52 ppm signal of the methylene carbon, show the same trend. But clearly, the smaller line width and better separation from other signals favors the analysis of cross-link densities to the 44 ppm signal.

Figure 6 displays the 44 ppm signal intensity as a function of the inverse chain segment M_n which is proportional to the cross-link density. A good linear correlation is observed, demonstrating the applicability of this analysis. For lower cross-link densities the values

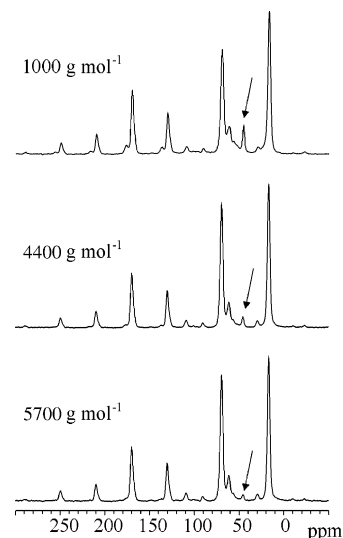


Figure 5. Stack plot of ^{13}C CPMAS spectra for polymer networks with different chain segment lengths. The number-average chain segment length of the samples is indicated next to the spectra. The arrows point at the 44 ppm signal whose intensity increases with increasing cross-link density. The spectra are scaled to the same signal intensity for the methyl signal. All polymer network chain segments have a lactide-to-glycolide molar ratio of 82:18.

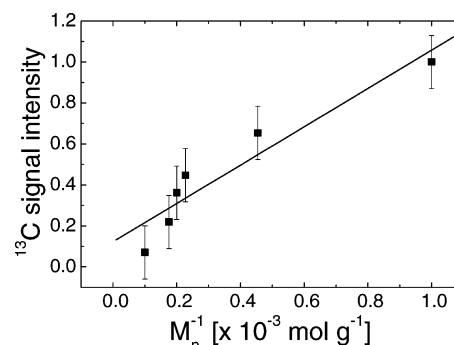


Figure 6. Intensity of the 44 ppm signal as a function of inverse chain segment length of the dimethacrylate precursor. The signal intensity is normalized to that of the sample with 1000 g mol^{-1} . All polymer network chain segments have a lactide-to-glycolide molar ratio of 82:18.

are slightly lower than the values expected from the regression line. Nonetheless, the analysis not necessarily reflects the absolute cross-link density. For a detailed characterization, a calibration with samples of well-defined cross-link density would be necessary. This would also require samples with uniform chain segment length rather than samples with a chain segment length distribution as in the described polymer networks. The almost linear dependence of signal intensity and inverse of chain segment M_n means that our analysis is applicable to determine relative cross-link densities within a sample series. Furthermore, our data for samples with varying chain segment length can be used as a calibration curve for these polymer network samples with unknown segment length or samples with higher polydispersities of the precursor. Of importance for application is the prediction of the degree of swelling of the polymer networks in a solvent which is also directly related to the cross-link density as can be followed by the signal intensity of the 44 ppm signal.

3.4. Cross-Link Density as a Function of UV Curing Time. The optimum time for UV curing is an important parameter for the synthesis of these polymer

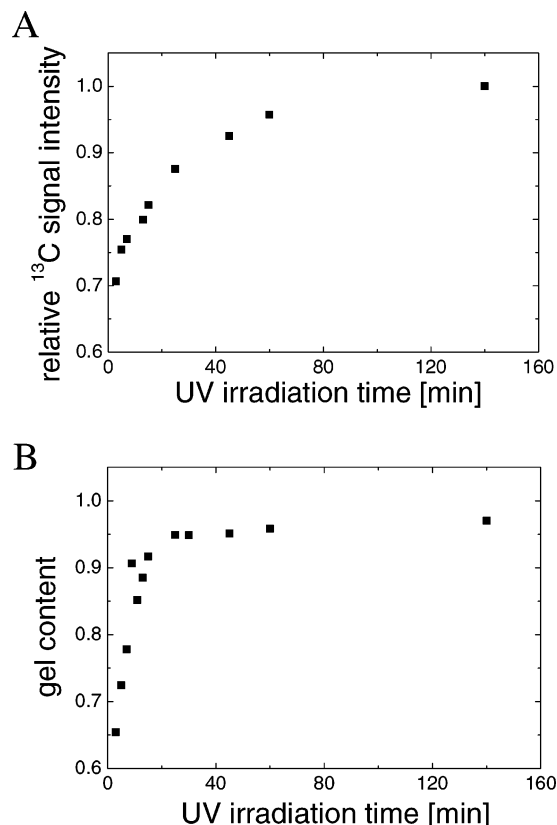


Figure 7. (A) Signal intensity of the 44 ppm signal in the ^{13}C CPMAS spectra of the polymer network as a function of UV curing time. The signal intensity is normalized to the signal intensity after 140 min. (B) Gel content of the polymer network as a function of UV curing time. The polymer network has a chain segment M_n of 5700 g mol^{-1} and a lactide-to-glycolide ratio of 71:29.

networks. If the time for photoirradiation is too short, cross-linking is incomplete and free chains and chain ends are present in the polymer network. But also, since UV light is of high energy, if irradiation is carried out for too long time periods, it could cleave or depolymerize the polymer chains and again reduce the cross-link density.

For a better control of the kinetics of the UV curing, polymer network samples were prepared that were exposed to the UV irradiation for different periods of time. Especially for precursors with higher molecular weight of the precursor incomplete reaction of all methacrylate end groups could happen due to a lower effective concentration of reactive groups. The progress of the UV curing process is followed as described in the previous section, by observing the intensity of the 44 ppm signal. To compare the results of different samples, one has to pay attention to use the same UV irradiation setup, i.e., lamp power, distance of sample to the lamp, heating effects due to the thermal radiation of the lamp, etc. Figure 7A shows representatively the cross-link density (displayed as the signal intensity of the 44 ppm signal) as a function of UV curing time for a sample with a precursor chain segment M_n of 5700 g mol^{-1} .

After 3 min of UV irradiation about 70% of the maximum signal intensity is already reached. Then the signal intensity is steadily increasing up to an irradiation time period of 140 min. This behavior can be explained as follows: at the beginning of photoirradiation methacrylate olefinic groups quickly react. Following this, the mobility of the network as well as of

unreacted methacrylate chain ends decreases, and therefore, at later stages, it becomes more and more unlikely for the oligomer units to "find" the reaction centers. Figure 7B represents the gel content as a function of irradiation time for the same polymer network sample. The gel content is defined as the ratio between the weight of the dried network after swelling and the weight of the network prior to extraction. From the comparison with Figure 7A it can be seen that the gel content increases faster with irradiation time than the corresponding signal intensity of the 44 ppm signal in the ^{13}C CPMAS spectrum. This is because the gel content depends on both chemical and physical cross-links, i.e., covalent bonds and entanglements or other constraints, respectively. Whereas the former are thermally stable, the latter are not and depend on the reaction conditions. In the ^{13}C CPMAS spectrum only the chemical cross-link density is determined which is a more accurate parameter to characterize the polymer network with respect to the progression of the UV reaction. It can also be seen that a gel content of 100%, i.e., quantitative reaction of all double bonds is not reached, because of the reduced mobility of the methacrylate bearing chain ends due to the increasing cross-link density of the polymer network.

The samples investigated in this work were irradiated for 25 min, although a slightly higher cross-link density can be obtained at longer irradiation times. More than 88% of the maximum cross-linking based on the ^{13}C CPMAS data has been reached. Incomplete cross-linking leaves over unreacted macrodimethacrylates as well as methacrylate chain ends from macrodimethacrylates which have only reacted at one end. Whereas the former are extracted by swelling the network as described above, the latter remain in the polymer network as freely dangling chains, thereby affecting the swelling behavior.

These results demonstrate the importance of using the optimum curing time. If the UV curing is incomplete, free methacrylate chain ends are present, and if UV curing was carried out too long, depolymerization by chain scission can occur although it was not observed here up to an irradiation time of 140 min. Both effects reduce the cross-link density directly. Further on this leads to an increased swelling which could be unfavorable for a given application.

3.5. Observation of the Shape-Memory Effect by Solid-State NMR. Typical experiments performed for testing the shape-memory properties of these polymer networks are cyclic thermomechanical tensile tests. In this investigation the possibility to use solid-state ^1H double quantum NMR spectroscopy to follow the shape-memory effect was examined. Double-quantum coherences are excited under nonspinning conditions using a general five-pulse sequence³⁰ including excitation and reconversion, and single-quantum intensity is observed as a function of double-quantum excitation time to yield so-called buildup curves. In general, the position of the maximum of double-quantum excitation reflects the strength of the dipolar coupling. The shorter the excitation time at the maximum of double-quantum coherence, the higher is the dipolar coupling. The programming of the polymer networks is done as follows: first, the sample is heated above T_g of the switching segment chains and stretched by a maximum elongation of 80%. The elongation is fixed by cooling the sample below T_g . Its shape is called the temporary shape. By heating the

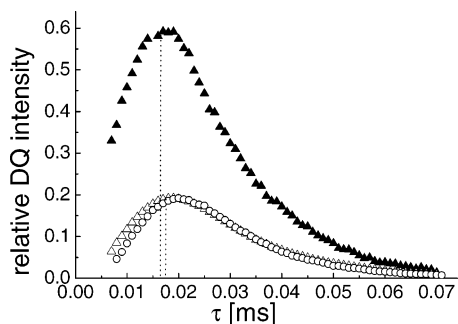


Figure 8. Double-quantum buildup curves of a polymer network with a lactide-to-glycolide molar ratio of 82:18 and a chain segment M_n of 4400 g mol⁻¹. An unstretched sample (open circles), a programmed sample with a maximum elongation of 80% (filled triangles), and the same sample after heating above T_g to recover the permanent shape (open triangles). The vertical dotted lines indicate the position of the maximum of double-quantum coherence for the stretched and unstretched samples. All measurements were performed at room temperature.

polymer network sample above T_g , the permanent shape can be recovered. The according double-quantum buildup curves are shown for a polymer network with a molar ratio of lactide to glycolide of 82:18 and a chain segment M_n of 4400 g mol⁻¹ in Figure 8. The intensity is normalized to the signal intensity of a standard one-pulse experiment with the same amount of scans. Because of the rigidity of the polymer network below T_g , a maximum is detected for the unstretched sample at an excitation time of 20 μ s. By stretching the sample, individual segments between the cross-linking points are elongated and partially oriented. Therefore, the dipolar coupling is increased which can be seen in Figure 8 by a shift in the buildup curve to a shorter time for the maximum of the curve at 18 μ s. Additionally, the normalized signal intensity is much higher for the stretched compared to the unstretched sample. This means that the efficiency of excitation of double-quantum coherence is strongly enhanced because of the higher dipolar coupling. After heating the polymer network sample above T_g without load, the permanent shape is recovered. A double-quantum measurement at room temperature shows an almost identical buildup curve compared to the unstretched sample. Thus, the shape-memory effect is reversible and can be followed by simple solid-state NMR methods. Unfortunately, the effect in the double-quantum experiment is not very pronounced due to two reasons. On one hand, the maximum elongation of these materials is below 100%; therefore, differences between dipolar couplings of the temporary and permanent shape are expected to be small. Further elongation leads to a break of the sample. On the other hand, the polymer network sample is already fairly rigid; therefore, the stretching does not influence the dipolar coupling too much. Nevertheless, the effect is clearly visible.

Another sample with the same composition programmed by applying a maximum elongation of 30% was also investigated by the double quantum method (data not shown). Because of the lower stretching ratio, the differences in the position of the maximum of the buildup curve and therefore the dipolar coupling strength between the samples with permanent and temporary shape were less pronounced, although still visible.

This experiment demonstrates that the programming of the temporary shape is reversible. In general, several

cycles have to be performed with programming and recovery to fully characterize the reversibility of the process.

4. Conclusions

It was demonstrated that solid-state NMR is a very useful tool to study chemical and physical properties of covalently cross-linked polymer networks. The networks in this study were obtained from UV cross-linking of a series of poly[(L-lactide-*ran*-glycolide)]dimethacrylates with different molecular weights of the precursor, resulting in polymer networks with different cross-link densities. By application of an appropriate programming, they exhibit shape-memory properties; i.e., a temporary macroscopic shape can be programmed which is recovered to the permanent shape at temperatures above T_g of the switching segment chains.

¹³C CPMAS spectra of these polymer networks and its synthetic precursors were completely assigned to all the molecular building units, including the signals from the methacrylate cross-linking point. Especially the signal at 44 ppm of the quaternary carbon of the formed poly(methacrylate) segments is well separated from all other signals. This enables a clear and simple calculation of its integral intensity and therefore the direct determination of the cross-link density. By application of this technique, the determination of the cross-link density as a function of chain segment length and optimum time of UV irradiation for cross-linking is possible. Furthermore, although CPMAS is not a quantitative method, it was shown that the relative ratio of the two monomers L-lactide and glycolide could be determined on the basis of the intensities of the methylene and methine carbons, yielding values close to the molar ratios from the synthesis input.

Comparison of the 44 ppm signal intensity and the gel content as a function of photoirradiation time of the polymer networks revealed that after a few minutes more than 70% of the cross-linking reactions had already taken place. After that, the gel content increased and reached a plateau value after roughly 25 min of photoirradiation while the ¹³C signal intensity at 44 ppm increased until the longest photoirradiation time of 140 min. Whereas the gel content is also influenced by entanglements and other physical constraints, the analysis of the 44 ppm signal intensity directly reflects the amount of covalent cross-links formed. Therefore, the ¹³C CPMAS technique is superior to the determination of the gel content.

The shape-memory effect could be observed by a ¹H double quantum experiment of the polymer network. A temporary shape produced by elongation of the sample by 80% revealed a higher dipolar coupling compared to the permanent shape. Afterward, the recovery to the permanent shape after heating the sample above T_g was observed to be almost completely reversible.

Consequently, solid-state NMR can be used efficiently to characterize polymer networks that are difficult to analyze otherwise. Especially the important parameter of cross-link density which determines the swelling behavior of the material could be quantified by the signal intensity of one of the ¹³C signals. In a practical application, a higher degree of swelling of the material increases its volume and may speed up the degradation of the implant. Therefore, the information from solid-state NMR can be employed to obtain implant materials that are tailored for a certain application. For similar

systems, we expect that solid-state NMR can also be employed successfully. A key feature of the analysis is its simplicity based on standard ^{13}C CPMAS spectra. Further investigation of these polymer networks on the temperature dependence of different NMR parameters as well as experiments on the degradation under physiological conditions will be presented in an upcoming publication.¹⁷

References and Notes

- (1) Langer, R.; Tirrell, D. A. *Nature (London)* **2004**, *428*, 487.
- (2) Laurencin, C. T.; Sobruasua, I. E. M.; Langer, R. S. In *Biomedical Applications of Synthetic Biodegradable Polymers*; Hollinger, J. O., Ed.; CRC: Boca Raton, FL, 1995; p 59.
- (3) Griffith, L. G. *Acta Mater.* **2000**, *48*, 263.
- (4) Okada, M. *Prog. Polym. Sci.* **2002**, *27*, 87.
- (5) Lendlein, A.; Langer, R. *Science* **2002**, *296*, 1673.
- (6) Lendlein, A.; Schmidt, A. M.; Schroeter, M.; Langer, R. *J. Polym. Sci., Polym. Chem.* **2005**, *43*, 1369.
- (7) Alteheld, A.; Feng, Y.; Kelch, S.; Lendlein, A. *Angew. Chem.* **2005**, *117*, 1212.
- (8) Li, S. J. *Biomed. Mater. Res.* **1999**, *48*, 342.
- (9) Jabbal-Gill, I.; Lin, W.; Kistner, O.; Davis, S. S.; Illum, L. *Adv. Drug Delivery Rev.* **2001**, *51*, 97.
- (10) Witschi, C.; Doelker, E. *J. Controlled Release* **1998**, *51*, 327.
- (11) Edelman, E. R.; Nathan, A.; Katada, M.; Gates, J.; Karnovsky, M. J. *Biomaterials* **2000**, *21*, 2279.
- (12) Ramchandani, M.; Robinson, D. J. *Controlled Release* **1998**, *54*, 167.
- (13) Lendlein, A.; Choi, N., manuscript in preparation.
- (14) Choi, N. *Degradable, Amorphous Networks for Medical Applications*. RWTH Aachen University, 1999.
- (15) Lendlein, A.; Kelch, S. *Angew. Chem.* **2002**, *114*, 2138.
- (16) Lendlein, A.; Kelch, S. *Angew. Chem., Int. Ed.* **2002**, *41*, 2034.
- (17) Buda, A.; Bertmer, M.; Blumenkamp-Höfges, I.; Kelch, S.; Lendlein, A., manuscript in preparation.
- (18) Stejskal, E. O.; Memory, J. D. *High-Resolution NMR in the Solid State*; Oxford University Press: New York, 1994.
- (19) Bennett, A. E.; Rienstra, C. M.; Auger, M.; Lakshmi, K. V.; Griffin, R. G. *J. Chem. Phys.* **1995**, *103*, 6951.
- (20) Opella, S. J.; Frey, M. H. *J. Am. Chem. Soc.* **1979**, *101*, 5854.
- (21) Alemany, L. B.; Grant, D. M.; Alger, T. D.; Pugmire, R. J. *J. Am. Chem. Soc.* **1983**, *105*, 6697.
- (22) Murphy, P. D. *J. Magn. Reson.* **1983**, *52*, 343.
- (23) Murphy, P. D. *J. Magn. Reson.* **1985**, *62*, 303.
- (24) Kasperczyk, J. *Polymer* **1996**, *37*, 201.
- (25) Kreiser-Saunders, I.; Kricheldorf, H. R. *Macromol. Chem. Phys.* **1998**, *199*, 1081.
- (26) Dobrzynski, P.; Kasperczyk, J.; Bero, M. *Macromolecules* **1999**, *32*, 4735.
- (27) Kalachandra, S.; Turner, D. T.; Burgess, J. P.; Stejskal, E. O. *Macromolecules* **1994**, *27*, 5948.
- (28) Edzes, H. T. *Polymer* **1983**, *24*, 1425.
- (29) Gilding, D. K.; Reed, A. M. *Polymer* **1979**, *20*, 1459.
- (30) Wokaun, A.; Ernst, R. R. *Chem. Phys. Lett.* **1977**, *52*, 407.

MA0501489